horticulturae

MDPI

Article

Morphological, Physiological and Biochemical Changes in the Grape Variety "Hotan Red" Caused by the Occurrence of Stress Under the Influence of Saline–Alkaline Growing Conditions

Yan Song [1], Ruxue Li [1,2], Long Zhou [1,*], Lili Jiang [3] and Xiong Wang [3]

[1] College of Horticulture, Xinjiang Agricultural University, Urumqi 830052, China; cliff_sy@163.com (Y.S.); liruxue2025@163.com (R.L.)
[2] Xinjiang Branch of the National Forest and Grass Germplasm Resources Facility Preservation Bank, Xinjiang Uygur Autonomous Region Forest and Grass Germplasm Resources Center, Urumqi 830000, China
[3] Forestry and Grassland Bureau of Awati County, Xinjiang Uygur Autonomous Region, Awati 843299, China; fanhuasayujll@163.com (L.J.); wx1213886393@163.com (X.W.)
* Correspondence: zhoulong2004@126.com

Abstract: The native Hotan Red grape germplasm from Xinjiang has strong saline–alkali tolerance. To clarify the physiological mechanisms of Hotan Red grapes in response to saline–alkali stress, Hotan Red hydroponic seedlings were used as the research material in this study and were subjected to the combined saline–alkali stress treatments of 0, 40, 80, 120 and 160 mmol·L^{-1}. After the 15th day of stress, plant height, shoot thickness, saline–alkali injury index, photosynthetic parameters, chlorophyll fluorescence parameters, osmoregulatory substance content, oxidation products and antioxidant enzymes of Hotan Red were determined. The results showed that the growth of plant height and shoot thickness of Hotan Red was inhibited, chlorophyll content decreased and the salinity damage index increased with increasing saline–alkali stress. Saline–alkali stress resulted in a non-stomatal limitation of photosynthesis in Hotan Red, which was manifested by a decrease in net photosynthetic rate, transpiration rate and stomatal conductance, and an increase in the concentration of intercellular carbon dioxide, in which the net photosynthetic rate reached a minimum value of 3.56 μmol·m^{-2}·s^{-1} under 120 mmol·L^{-1} saline–alkali stress; the actual photochemical efficiency of PSII in the light and maximal quantum yield of PSII decreased, with minimum values of 0.16 and 0.60, respectively. Accumulation of superoxide anion, hydrogen peroxide, malondialdehyde, proline, soluble sugars and soluble proteins, and enhancement of superoxide dismutase, catalase and peroxidase activities were observed in Hotan Red under saline–alkali stress. Partial least squares path model analysis showed that photosynthesis was the main driver of saline–alkali injury in Hotan Red, followed by oxidation products and antioxidant enzymes, with osmoregulators playing an indirect role. This study revealed the physiological mechanism by which Hotan Red tolerates saline–alkali stress, providing a basis for further research into the mechanism of saline–alkali tolerance in grapes.

Keywords: Hotan Red grape; saline–alkali stress; PLS-PM; morphology; physiological and biochemical response

Academic Editors: Susana González-Morales, Fabián Pérez Labrada, Yolanda González-García and Adalberto Benavides-Mendoza

Received: 17 December 2024
Revised: 3 January 2025
Accepted: 9 January 2025
Published: 10 January 2025

Citation: Song, Y.; Li, R.; Zhou, L.; Jiang, L.; Wang, X. Morphological, Physiological and Biochemical Changes in the Grape Variety "Hotan Red" Caused by the Occurrence of Stress Under the Influence of Saline–Alkaline Growing Conditions. *Horticulturae* **2025**, *11*, 69. https://doi.org/10.3390/horticulturae11010069

1. Introduction

Soil salinisation has become a pervasive issue affecting global resources and ecosystems. It represents a significant constraint on agricultural and environmental development. According to recent estimates, the global area of saline–alkali soil spans 950 million hectares,

representing approximately 20% of the world's agricultural land [1]. As a major agricultural country, China is confronted with a significant challenge in the form of soil salinisation, which is pervasive and spans an area of up to 99.133 million hectares. This has led to the impact of salinity on nearly 7.6 million hectares of crops [2]. Xinjiang has the distinction of possessing the largest area of saline–alkali land in the country, accounting for approximately one-third of the total cultivated land area [3]. By improving soil quality and enhancing crop tolerance to salinity and alkalinity, these regions still possess significant potential for agricultural development. The vigorous development and utilisation of indigenous crop germplasm represent a significant avenue for sustainable agricultural development.

Currently, most of the research on saline–alkali tolerance in crops focuses on neutral salinity tolerance, and research on compound saline–alkali stress is relatively limited. Soil salinity and alkalinity typically co-occur in natural ecosystems. A single salt or alkali stress does not fully elucidate the impact of saline–alkali environments on plants in field soils [4]. The effects of saline–alkali stress on plants are more detrimental than those of neutral salts. In addition to the challenges posed by osmotic stress and ionic toxicity, plants subjected to saline–alkali stress must also contend with high pH levels [4–7]. Therefore, exploring the mechanisms of crop tolerance to compound saline–alkali stresses is important for the development of strategies for saline–alkali land improvement and utilisation in Xinjiang.

Under saline–alkali stress, cellular oxidation is considered one of the major threats in plants. Studies have shown that saline–alkali stress causes plants to produce large amounts of reactive oxygen species (ROS), and these ROS trigger oxidative damage to cell membrane lipids, proteins and nucleic acids, leading to cellular dysfunction and even programmed cell death, which is visually manifested as leaf greenness, wilting and abscission [8–10]. Furthermore, there is a strong correlation between ROS accumulation and photosynthetic efficiency in both directions. It has been demonstrated that salinity stress causes electron leakage in the electron transport chain, which in turn results in the generation of reactive oxygen species (ROS) [11]. Another study demonstrated that the accumulation of ROS can result in the degradation of photosynthetic pigments, the obstruction of photosynthetic electron transfer and a reduction in photochemical efficiency [12]. It can be seen, therefore, that plants can scavenge ROS through antioxidants, which in turn reduces the negative impact on photosynthesis. To illustrate this, *Malus pumila* Mill. [13], *Actinidia chinensis* Planch. [14] and *Musa acuminata* cv. BD [15] scavenge ROS accumulation during saline–alkali stress through the activity of antioxidant enzymes and the expression levels of their associated genes. Furthermore, plants can enhance their tolerance to saline–alkali stress by accumulating proline (Pro), soluble sugars (SSs), and soluble proteins (SPs), which not only act as osmoregulators but are also involved in ROS scavenging processes [16,17].

Grapes (*Vitis vinifera* L.) are one of the most characteristic fruits of Xinjiang, with a long history of growing. The Xinjiang grape-growing area and its production constituted 17.16% and 20.58% of the country's total, respectively [18]. They play an important role in farmers' income and the adjustment of the agricultural industry structure. In recent years, to promote the grape industry's high-quality development, many high-quality varieties have been introduced into Xinjiang, such as the Shine-Muscat, Hu Tai series, Romantic Beauty and Summer Black. Although the majority of regions graft these high-quality varieties on rootstocks with strong adversity (e.g., Paulsen 1103, Richter 110 Sélection Oppenheim 4, etc.), it is still difficult for them to adapt to the saline soil environment in Xinjiang. This results in these high-quality varieties not being able to realise their maximum production capacity, which has a significant impact on the healthy development of the grape industry. Nevertheless, many native local grapes have been domesticated by natural selection over time, giving them saline–alkali tolerance, such as the Hotan Red grape. An illustrative example is the Hotan Red grape. Hotan Red belongs to the Eurasian grape,

which originated in China and is the main cultivated variety in the Hotan region of Xinjiang. It is a native variety with a long history of use in the region and can be employed in the production of fresh food, dried products and wine. Moreover, it possesses significant medicinal properties. For instance, it has been demonstrated to possess the capacity to inhibit the growth of stomach and liver cancer cells [19]. Furthermore, it serves as the primary constituent of the national medicinal liquor known as 'Musales'. The Hotan Red is widely distributed throughout the circum-Tarim Basin, where soil saline–alkali is a significant and long-standing issue [20]. The capacity of Hotan Red to flourish in such an environment indicates that it has exhibited an exceptional degree of saline–alkali tolerance. Nevertheless, the underlying physiological mechanism of saline–alkali tolerance in Hotan Red remains elusive. In light of the aforementioned considerations, the present study employed the Hotan Red as research material to investigate the evolving patterns of its morphological characteristics, photosynthetic parameters, osmotic regulation, ROS and antioxidant system in response to compound saline–alkali stress. Furthermore, the partial least squares path model (PLS-PM) was applied to analyse the drivers of saline–alkali damage in Hotan Red. Elucidating the physiological mechanisms of Hotan Red grapes in response to saline–alkali stress will be of great significance and offer broad application prospects for the genetic improvement of grapes against saline–alkali damage and the utilisation of saline–alkali land.

2. Materials and Methods

2.1. Plant Material and Treatments

At the Xinjiang Branch of the National Forest and Grass Germplasm Resources Facility Preservation Bank, tissue culture seedlings of Hotan Red with consistent growth were selected and acclimated hydroponically in the Hoagland medium (Beijing Suolaibao Technology Co., Ltd., Beijing, China). The temperature of the culture room was 25 ± 3 °C, the air humidity was 65 ± 2%, the light intensity was 4000–5000 Lx and the day and night length was 16 h/8 h. The seedlings were treated with combined salt–alkali stress when they had grown to 5–8 mature leaves. The molar concentration ratio of saline–alkali components in the soil of the main production area of Hotan Red ($NaCl$:Na_2SO_4:$NaHCO_3$ = 1:2.4:1.4) (Tianjin Zhiyuan Chemical Reagent Co., Ltd., Tianjin, China) was used as the basis for the preparation of the complex saline–alkali solution. Different concentrations of complex saline–alkali solution were prepared and added to the hydroponic solution to achieve saline–alkali stress in the hydroponic solutions of 0 mmol·L^{-1} (pH = 7.11, S0 or CK), 40 mmol·L^{-1} (pH = 8.06, S1), 80 mmol·L^{-1} (pH = 8.29, S2), 120 mmol·L^{-1} (pH = 8.41, S3) and 160 mmol·L^{-1} (pH = 8.63, S4). Every 5 days, we replaced the hydroponic solution. Each treatment was replicated with 30 plants and the determination of morphological and photosynthetic indices was started after 15 days. The leaves of all the hydroponically grown seedlings were then collected and, according to the different treatments, mixed pools of samples were prepared, treated with liquid nitrogen and stored in a refrigerator at −80 °C for the determination of physiological and biochemical indices.

2.2. Measurement of Morphological Indicators

Before the saline–alkali stress treatment, 3 seedlings with the same growth were randomly selected from each group, and the plant height (H, cm) and shoot diameter (D, mm) were measured using vernier callipers and straighteners (Shenzhen Shenzhu Precision Measuring Instrument Co., Ltd., Shenzhen, China). The saline–alkali damage index was determined according to the method of Du [21], and the saline–alkali damage criteria were divided into 5 levels: Level 0, no signs of saline–alkali damage; Level 1, mild saline–alkali damage, with a small part of the leaf tips, leaf margins or veins turning yellow; Level 2,

moderate saline–alkali damage, with more than half of the leaf tips, leaf margins or veins scorched; Level 3, severe saline–alkali damage, with most of the leaf blades scorched or defoliated and Level 4, very severe saline–alkali damage, with wilting, defoliation and plant death.

$$\text{Saline–alkali damage index} = \Sigma(\text{Saline–alkali hazard class} \times \text{Number of plants in the corresponding class})/(\text{Supreme class} \times \text{Total number of plants investigated})$$

2.3. Determination of Chlorophyll Fluorescence and Photosynthetic Parameters

The content of chlorophyll (ChI) was determined according to the method described by Hussain et al. [22]. Chlorophyll fluorescence parameters were determined using a Li-600 fluorescence-stomatometer (Li-Cor, Tucson, AZ, USA), and after 20 min of dark adaptation, fluorescence parameters were measured and calculated for fully developed leaves of Hotan Red morphology from the bottom upwards of the 3rd–5th leaf. The instrument can directly measure parameters such as onset fluorescence (F_o), maximum fluorescence (F_m), steady-state fluorescence (F_s), maximum fluorescence signal (Fm') and minimum fluorescence (F_o'). The actual photochemical efficiency of PSII in the light ($\varphi PSII$), the maximum light energy conversion efficiency (F_v/F_m) and the non-photochemical quenching coefficient (NPQ) were calculated as follows.

$$\varphi PSII = (F_m' - F_s)/F_m'$$

$$F_v/F_m = (F_m - F_o)/F_m$$

$$NPQ = F_m/F_m' - 1$$

Net photosynthetic rate (Pn), transpiration rate (Tr), stomatal conductance (Gs) and intercellular carbon dioxide content (Ci) of fully developed leaves of Hotan Red from bottom to top were determined using the GFS-3000 (Walz, Nuremberg, Germany). As the hydroponic seedlings were inside the growth chamber and could not be moved, a red and blue LED light source (light intensity set at 1500 $\mu mol \cdot m^{-2} \cdot s^{-1}$) was used to simulate light.

2.4. Determination of Osmotic Regulators

Following the method of Zhao et al. [23], at 15 days after treatment, the 3rd–5th fully developed leaves of Hotan Red were collected from the bottom up and rinsed with deionised water, and then 10 leaf discs were taken with a perforator of 1 cm diameter, placed in a centrifuge tube, filled with 5 mL of deionised water, sealed and left to stand for 12 h. The initial conductivity (S1) was measured with a conductivity metre (Shanghai Yidian Scientific Instrument Co., Ltd., Shanghai, China). The centrifuge tubes were sealed, boiled in a water bath for 20 min and cooled to room temperature and then the final conductivity (S2) and the blank conductivity (S0) were determined, the blank conductivity being the conductivity of ionised water. The relative electrical conductivity (REC) was calculated using the following formula.

$$\text{REC}\ (\%) = (\text{S1} - \text{S0}) \times 100/(\text{S2} - \text{S0}) \quad (1)$$

The proline (Pro) content was determined using the method of Vieira et al. [24]. A total of 10 mL of the sample was fixed to 200 mL with purified water, 1 mL was pipetted and transferred to a test tube, 1 mL of formic acid (Guangdong Wengjiang Chemical Reagent Co., Ltd., Shaoguan, China) and 2 mL of 2,2-dihydroxyindane-1,3-dione (Beijing KangRenNa Biotechnology Co., Ltd., Beijing, China) were added sequentially and mixed and the bath of boiling water was applied for 15 min. When it had cooled down, 10 mL of

n-butyl acetate (Jiangsu Bosite Chemical Technology Co., Ltd., Nantong, China) was added and mixed well. The organic phase was filtered through sodium sulphate filter paper and the Pro concentration was determined spectrophotometrically.

In total, 0.1 g of leaf samples were weighed, 1 mL of distilled water was added and the mixture was ground to homogeneity, and then processed at 95 °C for 10 min (sealed to prevent water loss), cooled to room temperature and centrifuged at 8000× *g* for 10 min at room temperature, with the supernatants taken as surrogate samples. The soluble sugar content of the surrogate samples was determined using the Plant Soluble Sugar Content Assay Kit (Beijing Boxbio Science and Technology, Beijing, China).

Protein content was determined using the BCA method of Campion et al. [25]. Protein standards (Beijing Biolebo Technology Co., Ltd., Beijing, China) of 0–100 μg were prepared and fixed at 100 μL with H_2O_2 (Nanjing Shengqinghe Chemical Co., Ltd., Nanjing, China), with 100 μL of pure water defined as blank. A total of 2 mL of BCA working solution (Shanghai Jingke Chemical Technology Co., Ltd., Shanghai, China) was added to tubes containing 100 μL of the sample (3 biological replicates per treatment), standard and blank, respectively, and mixed thoroughly. The tubes were incubated at 60 °C for 15 min and cooled to room temperature, and the absorbance of the sample solution was determined spectrophotometrically. The soluble protein content of the sample was determined from the standard curve.

2.5. Determination of Oxidation Product Content and Antioxidant Enzyme Activity

Peroxidase (POD) activity was determined according to the method of Wang et al. [26]. A total of 1 mL of 50 mM potassium phosphate buffer (pH 7.0) (Shanghai Aiyan Biotechnology Co., Ltd., Shanghai, China) was added to 1 g of the sample with grinding to homogeneity, and then centrifuged, with 0.01 mL of supernatant obtained, and 10 mM phosphate buffer, 20 mM guaiacol (Shanghai Jingke Chemical Technology Co., Ltd., Shanghai, China) and 40 mM H_2O_2 added and shaken well. The reaction was stopped by the addition of 5% metaphosphoric acid (Shanghai Aiyan Biotechnology Co., Ltd., Shanghai, China) after 10 min and the photometric values were measured spectrophotometrically to calculate the POD activity. Catalase (CAT) activity was determined using the method of Song et al. [27]. SOD enzyme activity was measured using a Superoxide Dismutase (SOD) Activity Assay Kit (Beijing Boxbio Science and Technology, Beijing, China). Malondialdehyde (MDA) was determined with the thiobarbituric acid (TBA) method according to Song et al. [27]. In total, 2 mL of 0.05 mol·L^{-1} phosphate buffer was added to 0.3 g of the sample and ground to a homogenate. It was transferred to a test tube and the mortar was washed with 3 mL of 0.05 mol·L^{-1} phosphate buffer. The extract was mixed thoroughly with 5 mL of 0.5% TBA (Beijing Boaosen Biotechnology Co., Ltd., Beijing, China). The tubes were immediately transferred to the ice water bath after 10 min in a boiling water bath. After cooling, the tubes were centrifuged at 3000× *g* for 15 min, the supernatant was removed and the malondialdehyde content was determined spectrophotometrically.

2.6. Statistical Analysis and Visualisation of Data

Morphological, physiological and biochemical data were analysed with the least significant difference (LSD) method using DPS v18.10 (Hangzhou Ruifeng, Hangzhou, China), and differences in $p < 0.05$ were considered statistically significant. The partial least squares path model (PLS-PM) was used to explore the components of the saline–alkali damage index due to the small sample size of the study and some covariance between variables. The PLS-PM model was constructed using the plspm R package (The R Programming Language 4.4.1, Auckland, New Zealand). The model included the following variables: osmoregulatory substances (REC, Pro, SS, SP), oxidation products and antioxidant enzyme

activities (SOD, POD, CAT, $O_2 \cdot^-$, MDA, H_2O_2), chlorophyll fluorescence parameters (ChI, F_o, F_m, F_v/F_m, $\varphi PSII$, NPQ) and photosynthetic parameters (Pn, Tr, Gs, Ci). Histograms were plotted using Origin 2018 (OriginLab, Northampton, MA, USA) and PLS-PM was visualised using Microsoft Office PowerPoint 2021 (Microsoft, Redmond, WA, USA).

3. Results

3.1. Effects of Saline–Alkali Stress on Morphological Characteristics of Hotan Red

As illustrated in Figure 1a, the Hotan Red cultivar exhibited a gradual loss of green colouration, wilting and leaf shedding in response to increasing saline–alkali stress. Following the S4 treatment, a significant proportion of the plants exhibited signs of death after 15 days. As illustrated in Figure 1b, both plant height (H) and shoot thickness (D) tended to decrease with increasing saline–alkali stress and were significantly ($p < 0.05$) lower than the control (S0) under both S3 and S4 treatments. In the case of H, S4 had the highest decrease ratio from the control, at 16.25%; the overall trend was the largest for S2, at 7.41%. Under the S4 treatment, Hotan Red had the highest D reduction ratio of 22.06%. Figure 1c illustrates the saline–alkali damage index, which, in conjunction with Figure 1a, demonstrates that the saline–alkali damage phenomenon becomes increasingly severe with elevated saline–alkali stress. The greatest increase in the saline–alkali damage index was observed in Hotan Red under S2 treatment, with a 300% increase from S1. The synthesis of morphological characteristics showed that the morphological characteristics of Hotan Red after the S1 treatment changed less compared to the control, while the morphological characteristics of Hotan Red after S2, S3 and S4 treatments changed more compared to the control. This indicates that, at the morphological level, the S1 treatment is the lowest tolerance threshold for saline–alkali in Hotan Red grapes.

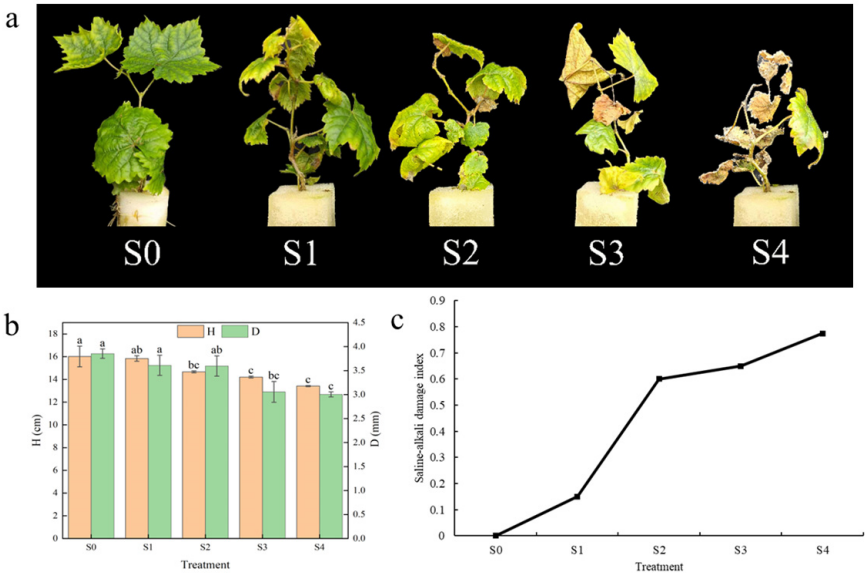

Figure 1. Effects of different saline–alkali stresses on morphological characteristics of Hotan Red. (**a**) The morphology of Hotan Red was observed following the application of various saline–alkali stress treatments; (**b**) plant height and shoot thickness of Hotan Red under saline–alkali stress. Different lowercase letters in the graphs indicate significant differences between treatments at the $p < 0.05$ level; (**c**) the saline–alkali damage index of Hotan Red under saline–alkali stress conditions.

3.2. Effects of Saline–Alkali Stress on Photosynthetic Parameters of Hotan Red

Photosynthesis is an important metabolic process in plants and is the basis for the synthesis of matter and energy. Figure 2 shows the photosynthetic parameters of Hotan Red grape leaves after different saline–alkali stress treatments (Because the saline–alkali

damage of Hotan Red after S4 treatment was too severe to measure the relevant indexes, the same as below). As saline–alkali stress increased, the net photosynthetic rate (*Pn*), transpiration rate (*Tr*) and stomatal conductance (*Gs*) exhibited a downward trend, while the change in interstitial carbon dioxide concentration (*Ci*) demonstrated an upward trend. As seen in Figure 2a, there were significant differences in *Pn* and *Tr* of Hotan Red leaves among treatments, with the lowest *Pn* and *Tr* of 3.56 μmol·m^{-2}·s^{-1} and 0.63 mmol·m^{-2}·s^{-1}, respectively, after S3 treatment. As seen in Figure 2b, the *Ci* of Hotan Red was significantly higher than that of the control in both S2 and S3 treatments, with 76.93% and 122.73% increases over the control, respectively. The *Gs* after S1, S2 and S3 treatments were significantly lower than the control, by 7.76, 47.75 and 64.56%, respectively. In summary, there were significant differences in the photosynthetic parameters of Hotan Red since the S2 and S3 treatments, and the magnitude of changes in each parameter was smaller after the S1 treatment. This indicates that, as far as the photosynthetic level is concerned, the S1 treatment is the lowest tolerance threshold for saline–alkali in Hotan Red grapes.

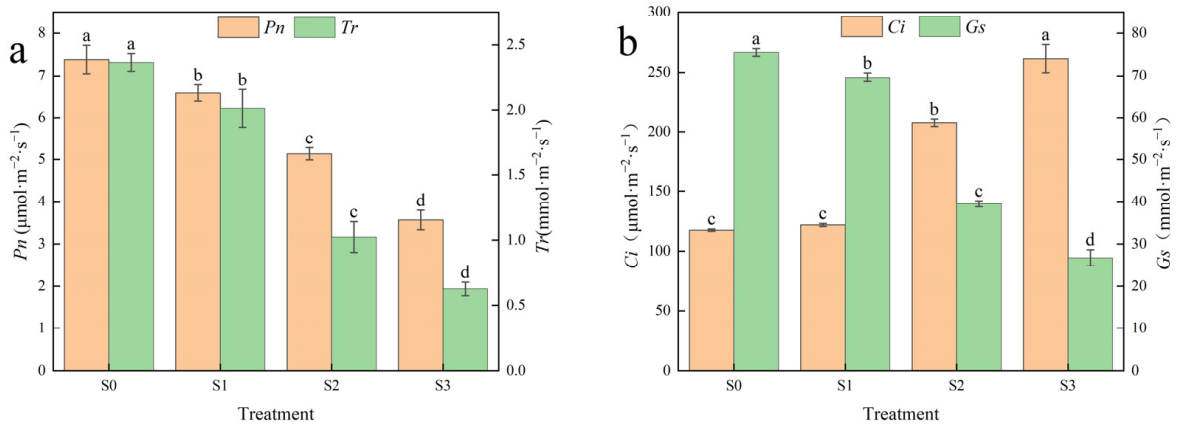

Figure 2. Effects of different saline–alkali stresses on photosynthetic parameters of Hotan Red. (**a**) The net photosynthetic rate (*Pn*) and transpiration rate (*Tr*) of 'Hotan Red' leaves after different saline-alkali stress treatments; (**b**) The intercellular carbon dioxide concentration (*Ci*) and stomatal conductance (*Gs*) of 'Hotan Red' leaves after treatment Different lowercase letters in the graphs indicate significant differences between treatments at the $p < 0.05$ level.

3.3. Effect of Saline–Alkali Stress on Chlorophyll Content and Fluorescence Parameters of Hotan Red

As can be seen in Figure 3a, the chlorophyll (ChI) content tended to decrease with increasing saline–alkali stress leading to the treatments, and ChI was significantly lower than that of the control under S1, S2 and S3 treatments, with ChI after S3 treatment being 0.85 times higher than that of the control (0.87 mg·g^{-1}). In addition, there was no significant difference in ChI between S1 and S2 treatments. It indicated that Hotan Red ChI increased the decomposition rate with increased saline–alkali stress. To further elucidate the extent of chloroplast damage under saline–alkali stress, chlorophyll fluorescence parameters were determined in this study. The results showed (Figure 3a) that the initial fluorescence (F_o) showed an increasing trend in contrast to ChI, and F_o was significantly higher than the control in all treatments at 126.05, 138.58 and 140.61, respectively. Maximum fluorescence (F_m) showed a decreasing trend with increasing saline–alkali stress, with F_m under S2 and S3 treatments being significantly lower than that of the control, whereas there was no significant difference in F_m between S1 and the control and between S2 and S3 treatments, with F_m under the S1 treatment being reduced by only 2.64% compared to the control. The actual photochemical efficiency of PSII in the light ($\varphi PSII$) indicates the actual photochemical efficiency of PSII in the light after partial closure of the PSII reaction centre under illuminated conditions and reflects the efficiency of light energy use. As seen in Figure 3b,

φPSII showed a decreasing trend with increasing saline–alkali stress, and *φPSII* was significantly lower than that of the control under both S2 and S3 treatments, with decreases of 63.04% and 74.20%, respectively, while the difference between *φPSII* and control under S1 treatment was not significant and only decreased by 6.63%. The maximal quantum yield of PSII (F_v/F_m) reflects the maximum conversion efficiency of primary light energy in the PSII reaction centre and is an effective indicator of the degree of photoinhibition. The trend of F_v/F_m as affected by saline–alkali stress was similar to that of *φPSII*, with F_v/F_m in both S2 and S3 treatments being significantly lower than in the control at 0.62 and 0.60, respectively. The non-photochemical quenching coefficient (*NPQ*) reflects the photoprotective capacity of the leaves. With increasing saline–alkali stress, the *NPQ* showed an 'N'-type trend, reaching a maximum value of 1.16 after S1 treatment.

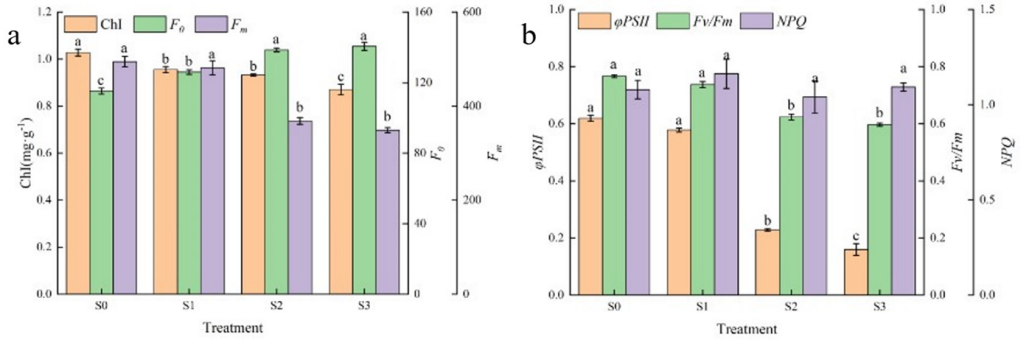

Figure 3. Effect of different saline–alkali stresses on chlorophyll content and fluorescence parameters of Hotan Red. (**a**) It shows the chlorophyll (ChI) content, initial fluorescence (F_o) and maximum fluorescence (F_m) of Hotan Red leaves after different saline–alkaline stress treatments; (**b**) it shows the actual photochemical efficiency of PSII in the light of PSII (*φPSII*), the maximum light energy conversion efficiency of PSII (F_v/F_m) and the non-photochemical quenching coefficient (*NPQ*). Different lowercase letters in the graphs indicate significant differences between treatments at the $p < 0.05$ level.

3.4. Effects of Saline–Alkali Stress on Osmoregulation in Hotan Red

As can be seen in Figure 4a, the relative conductivity (REC) and proline (Pro) content tended to increase with increasing saline–alkali stress. The REC varied significantly among the treatments with increases of 42.31, 54.78 and 63.12 percent, respectively, compared to the control. Pro content, under S1, S2 and S3 treatments, was significantly higher than the control, reaching a maximum value of 27.60 μg·g^{-1} with an increase of 203.41% under S3 treatment, while Pro under S1 and S2 treatments increased by 75.78% and 118.85% as compared to the control. Figure 4b shows the soluble sugar (SS) content and soluble protein (SP) content of Hotan Red leaves after treatment. The SS content showed an increasing and then decreasing trend with increasing saline–alkali stress, reaching a peak of 5.31% under the S2 treatment, which was nearly 138.46% higher than the control. In addition, SS content in the leaves of Hotan Red was significantly higher than that of the control after each saline–alkali stress treatment, and the changes were large, and only the S1 treatment increased the SS content by 105.88% compared with that of the control. The trend of SP content with increasing saline–alkali stress was similar to that of SS content, first increasing and then decreasing, and also reaching a peak value of 14.01 mg·g^{-1} under S2 treatment. The SP content under all treatments was significantly higher than under the control, with increases of 115.12%, 222.10% and 211.99%, respectively, compared to the control. In summary, with the increase in saline–alkali stress, osmoregulatory substances in the leaves of Hotan Red accumulate in large quantities in response to the damage caused by osmotic stress to the plant.

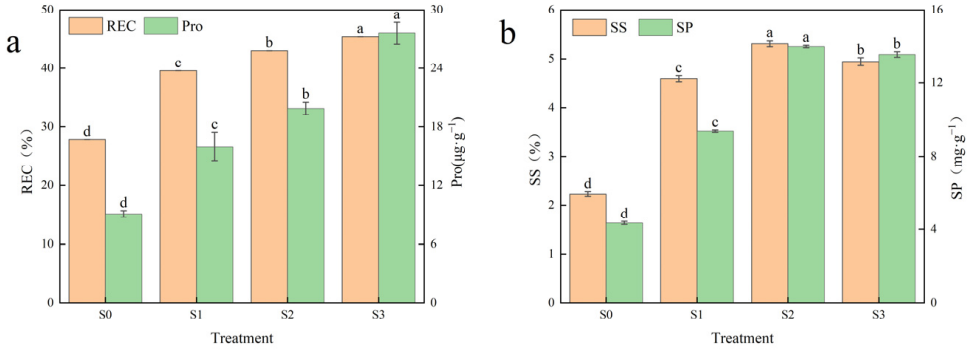

Figure 4. Effect of different saline–alkali stresses on osmoregulation in Hotan Red. (**a**) It shows the relative electrical conductivity (REC) and proline (Pro) content of Hotan Red leaves after different saline–alkali stress treatments; (**b**) it shows the soluble sugar (SS) content and soluble protein (SP) content of 'Hotan Red' leaves after treatment. Different lowercase letters in the graphs indicate significant differences between treatments at the $p < 0.05$ level.

3.5. Effect of Saline–Alkali Stress on Oxidation Products of Hotan Red

Malondialdehyde (MDA) and reactive oxygen species (ROS) are both products of the peroxidation of cellular structures when plants are exposed to stress and are key signalling molecules that enable cells to respond rapidly to various stimuli, with ROS including superoxide anions ($O_2 \cdot^-$) and hydrogen peroxide (H_2O_2). As can be seen in Figure 5, saline–alkali stress led to an increase in MDA content by, 7.63%, 51.61% and 104.05%, respectively, which was significantly higher than the control under S2 and S3 treatments. The H_2O_2 content was significantly higher under all saline–alkali stress treatments with increases of 22.31%, 74.40% and 174.72%, respectively. With the elevation of saline–alkali stress $O_2 \cdot^-$ content showed an increasing trend, reaching a maximum value of 11.42 nmol·g^{-1} under S3 treatment, with an increase of 162.82%. Although the difference between $O_2 \cdot^-$ under S1 treatment and the control was not significant, the increase was nearly 24.50% over the control.

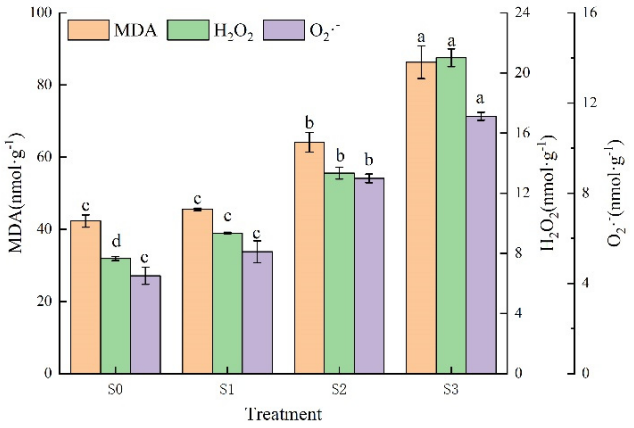

Figure 5. Effect of different saline–alkali stresses on oxidation products of Hotan Red. Different lowercase letters in the graphs indicate significant differences between treatments at the $p < 0.05$ level.

3.6. Effects of Saline–Alkali Stress on Antioxidant Enzyme Activities of Hotan Red

Catalase (CAT) is an anti-ageing protective enzyme of organisms that maintains the stability and integrity of cell membranes and catalyses the decomposition of H_2O_2 into O_2 and H_2O. As shown in Figure 6, with increased saline–alkali stress, CAT activity showed an increasing trend, reaching a maximum value of 121.58 μmol·min^{-1}·g^{-1} under S3 treatment, which was significantly higher than that of control; CAT activity under S1 and S2 treatments was not significantly different from that of the control, but increased by 20.96% and 57.69%,

respectively, compared with the control. Peroxidase (POD) catalyses the reaction between H_2O_2 and other substrates and has the effect of eliminating H_2O_2. POD activity in the leaves of Hotan Red showed an increasing trend under saline–alkali stress and was significantly higher than the control under S2 and S3 treatments, with increases of 209.48% and 243.16%, respectively, whereas there was no significant difference between S1 and the control, and between S2 and S3. Superoxide dismutases (SOD) are a class of enzymes that catalyse the disproportionation of $O_2 \cdot^-$ to H_2O_2 and O_2. With the elevation of saline–alkali stress, SOD activity showed an increasing trend and was significantly higher than the control under all treatments. The S3 treatment reached the highest value of 166.73 $U \cdot g^{-1}$, which increased by 136.43% from the control and was 3.08 and 1.83 times higher than the increase in SOD activity under the S1 and S2 treatments, respectively.

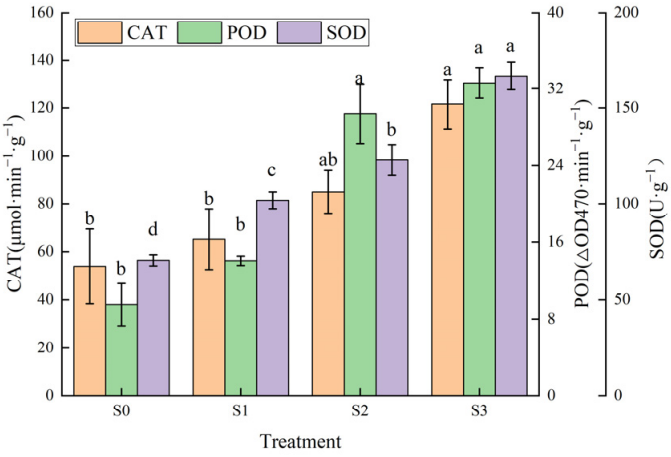

Figure 6. Effect of different saline–alkali stresses on antioxidant enzyme activities of Hotan Red. Different lowercase letters in the graphs indicate significant differences between treatments at the $p < 0.05$ level.

3.7. Partial Least Squares Path Modelling Analysis of the Components of the Saline–Alkali Damage Index in Hotan Red

To further explore the drivers of the saline–alkali damage index in Hotan Red, all the observed variables in this study were divided into four hidden variables, namely osmoregulatory substances, ROS and antioxidant enzyme systems, chlorophyll fluorescence parameters and photosynthetic parameters. Based on this, the partial least squares path model (PLS-PM) was constructed. As can be seen in Figure 7, the loading coefficients on the hidden variables are all greater than 0.85 for each of the observed variables (except for *NPQ*), indicating that the selected observed variables characterise their hidden variable significance well. The variables were able to explain the saline–alkali damage index well, and the overall goodness of fit of the model was 0.91, which is an overall good performance. The saline–alkali gradient had highly significant negatively correlated effects ($p < 0.001$) on osmoregulatory substances (−0.95), ROS and antioxidant enzyme systems (−0.98), chlorophyll fluorescence parameters (−0.96) and photosynthesis parameters (−0.98), and indirectly on the saline–alkali damage index (0.96), respectively. Negative correlations were found between combinations of latent variables, except for the positive correlations between oxidation and antioxidant enzyme systems and osmoregulatory substances (0.88), and chlorophyll fluorescence parameters and photosynthetic parameters (0.96). In addition, the saline–alkali damage index was significantly negatively correlated ($p < 0.05$ or $p < 0.001$) with the chlorophyll fluorescence parameter (−0.71), the oxidation and antioxidase (−0.76) and the photosynthetic parameter (−0.95), respectively.

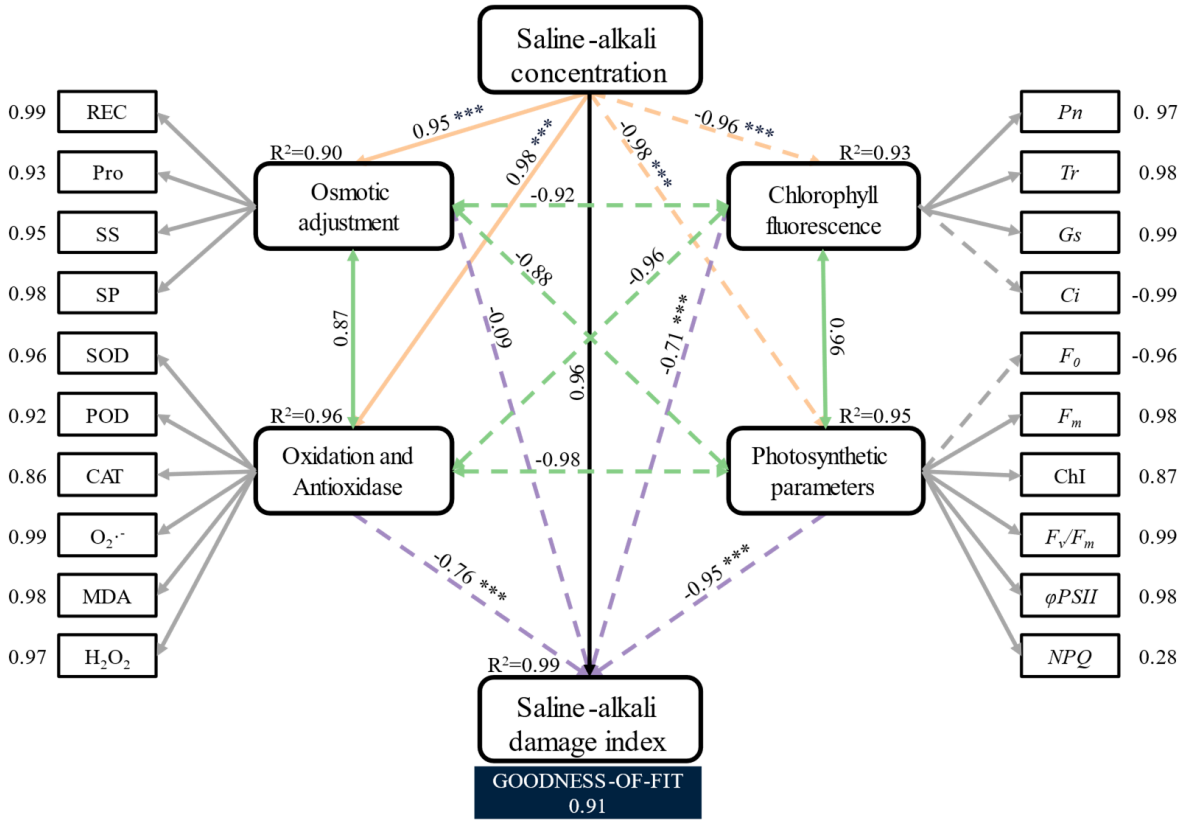

Figure 7. Partial least squares path model analysis of the drivers of the saline–alkali damage index of Hotan Red. The partial least squares path model (PLS-PM) shows the relationship between four latent variables, osmoregulatory substances, oxidative and antioxidant enzymes, chlorophyll fluorescence parameters and photosynthetic parameters and the saline–alkali damage index. In the figure, the orange line shows the effect of the saline–alkali treatments on the latent variables, the purple line shows the relationship between the latent variables and the saline–alkali damage index, the green pigmented line shows the interrelationships between the latent variables in the model, the grey line shows the loading coefficients between the latent variables and the observed variables in the model and the solid and dashed lines show the positive and negative path coefficients, respectively. R^2 is the coefficient of determination of the paths, with a significance level of *** ($p < 0.001$), and the goodness of fit of the model is 0.91.

4. Discussion

Saline–alkali stress impairs plant growth, and plants have evolved regulatory mechanisms to adapt to saline–alkali stress through self-selection, e.g., by actively slowing their growth rate to improve survival under saline–alkali damage. Therefore, the slowing of the aboveground growth rate and the reduction in plant height are undoubtedly the most intuitive manifestations of saline–alkali stress in plants, and also the most effective adaptive strategies of plants to saline–alkali stress [28]. Yu et al. [29] found that saline–alkali stress resulted in the wilting and shrivelling of leaves and a significant reduction in the growth of shoots. Furthermore, the survival of plants is contingent upon the saline–alkali content of the environment. It has been reported that the height, stem thickness and leaf area of Cabernet Sauvignon grapevine seedlings decreased with increasing saline–alkali stress concentrations [30]. Similarly to the results, Hotan Red showed a series of saline–alkali damage symptoms such as leaf greenness, wilting and abscission in varying degrees as the saline–alkali gradient increased. Saline–alkali stress accelerates the decomposition of chlorophyll and is one of the most important factors leading to leaf yellowing. As the most important and effective pigment in photosynthesis, chlorophyll is involved in the

absorption, transmission and conversion of light energy, and its content is an important indicator of the strength of photosynthesis [31]. Xu et al. [32] demonstrated that the exposure of grape leaves to saline–alkali stress resulted in a range of physiological changes, including yellowing and wilting, and a consequent decrease in the photosynthetic rate. The chlorophyll content in the leaves of Hotan Red decreased significantly with increasing saline–alkali gradient, in agreement with the study on Cabernet Sauvignon grapes by Qin et al. [33]. This suggests that saline–alkali stress may have disrupted the chloroplast structure of Hotan Red and increased chloroplast enzyme activity, which accelerated the degradation of photosynthetic pigments. In addition, oxidative damage to chloroplasts due to saline–alkali stress leads to a significant decrease in the rate of CO_2 assimilation and a non-stomatal limitation of photosynthesis [34].

Saline–alkali stress affects photosynthesis in the grapevine in two ways: leaf stomatal limitation and non-stomatal limitation, which changes from stomatal limitation to non-stomatal limitation with increasing saline–alkali stress concentration and duration [35,36]. In general, plants respond to early saline–alkali stress damage by closing stomata, reducing leaf water potential and inhibiting the rate of upward Na^+ transport [37,38]. As the stress duration and intensity increased, the main factors for the decrease in photosynthetic rate came from non-stomatal limitations, such as the increase in the impedance of chloroplasts to allow stomatal diffusion, the decrease in CO_2 solubility, the decrease in the affinity of Ribulose-1,5-bisphosphate carboxylase (Rubisco) for CO_2 and the decrease in the regeneration capacity of Ribulose-1,5-bisphosphate (RuBP) [39–41]. Research has demonstrated that exposure to saline–alkali stress results in the decline in Rubisco activity and subsequent inhibition of photosynthetic capacity in grape leaves [42]. Song et al. [43] found that Paulsen 1103, Richter 110 and Sélection Oppenheim 4 photosynthetic characteristics were negatively affected by increasing saline–alkali concentration. In the present study, we found that the net photosynthetic rate (*Pn*), transpiration rate (*Tr*) and stomatal conductance (*Gs*) of Hotan Red significantly decreased with increasing stress intensity, and the intercellular carbon dioxide concentration (*Ci*) showed an increasing trend, which is in agreement with the results of Martin [42], Zhu [44] and Shankar et al. [45] on *Vitis vinifera* L., *Malus pumila* Mill. and *Citrus sinensis* (L.) Osbeck. This suggests that Hotan Red suffered a reduction in photosynthesis rate due to non-stomatal limitation at 15 days of stress. At the same time, it indirectly reflected that the photosynthetic organs of Hotan Red were damaged by saline–alkali stress. Chlorophyll fluorescence parameters can be used to assess damage to photosynthetic organs under stress, and studies have shown that saline–alkali stress causes chloroplast swelling, an increase in the number and size of plastid globules and the disruption of cystoid membranes, leading to the structural disruption of photosynthetic organs [46]. Changes in the actual photochemical efficiency of PSII in the light (*φPSII*) and maximal quantum yield of PSII (F_v/F_m) can indicate how the plant photosynthetic system is affected by stress, particularly in terms of the extent of damage to the PSII rFeaction centre [46,47]. It was found that φPSII and F_v/F_m were significantly reduced in *Vitis vinifera* L. [36], *Pyrus species* [48] and *Olea europaea* L. [49] after saline–alkali treatment. Similarly to these results, *φPSII* and F_v/F_m decreased with increasing saline–alkali gradient in Hotan Red leaves. This suggests that saline–alkali stress negatively affected the function of the PSII reaction centre of Hotan Red and that the effect may be a stress-induced structural change or dysfunction. In addition, saline–alkali stress activates plant photoprotective mechanisms, such as the non-photochemical quenching coefficient (*NPQ*), to protect PSII reaction centres from damage [46]. It was found that the *NPQ* of grape leaves increased under salt stress conditions and decreased under alkali stress conditions [50]. In contrast, the present study found that the *NPQ* of Hotan Red leaves first increased and then decreased with the combined saline–alkali gradient, peaking at 40 mmol·L^{-1} saline–alkali

treatment. This suggests that long-term exposure of Hotan Red to a saline–alkali gradient of 40 mmol·L^{-1} can reduce the loss suffered by PSII due to the *NPQ*, whereas if the intensity of saline–alkali stress is too high, it leads to excessive losses suffered by the photosystem and inhibits the operation of photoprotective mechanisms. Therefore, the saline–alkali gradient concentration of 40 mmol·L^{-1} is the lowest tolerance threshold for Hotan Red in terms of photosynthetic physiology.

Osmotic stress is one of the main responses of plant cells to saline–alkali stress, and the resulting secondary oxidative stress, which also leads to photosynthetic physiological damage, ultimately constrains yield and quality [51]. Under saline–alkali stress, organic osmoprotectants such as proline (Pro), soluble sugars (SSs) and soluble proteins (SPs) maintain the osmotic balance between the cellular protoplasts and the external environment, protecting protein activity and cell membrane structure [52,53]. Chen et al. [54] found that saline–alkali stress induced the accumulation of osmoregulatory substances such as Pro, SSs and SPs in grape leaves. In this study, we found that Hotan Red regulates the osmotic pressure inside and outside the cell by increasing the contents of Pro, SSs and SPs in the leaves, which in turn reduces the damage brought by osmotic stress, as well as its secondary oxidative stress, to the cell structure and organelles. Our results are consistent with those of Wei [16], Oliveira [55] and Guo [56] on *Musa acuminata* cv. BD, *Hylocereus costaricensis* and *Asparagus officinalis* L. The membrane system of plants is the first part of the cell to sense saline–alkali stress when damage to the cell membrane is mainly manifested by membrane lipid oxidation reactions [57]. Malondialdehyde (MDA) is a membrane lipid peroxidation product, and the accumulation of MDA can reflect the potential antioxidant capacity of the organism and, indirectly, the degree of peroxidative damage to cell membranes [58]. It was shown that the MDA content of the salt-tolerant variety Richter 110 was significantly higher under salt stress conditions [52]. In the present study, it was found that saline–alkali stress resulted in a gradual increase in the MDA content of Hotan Red, which is consistent with the results of Li [59], Marie [60] and Wang's [61] studies on four varieties of *Vitis vinifera* L., *Poncirus trifoliata* L. and *Malus pumila* Mill. The accumulation of MDA also affects cells in the opposite direction, leading to an imbalance in the intracellular reactive oxygen species (ROS) system [62]. In Tamina grape leaves, ROS such as hydrogen peroxide (H_2O_2) and superoxide anions ($O_2\cdot^-$) increased with saline–alkali stress [63]. Our results were similar to those in that saline–alkali stress caused H_2O_2 and $O_2\cdot^-$ accumulation in Hotan Red cells. Antioxidant enzymes are one of the mechanisms for scavenging ROS and include mainly superoxide dismutase (SOD), catalase (CAT) and peroxidase (POD). SOD, as the first line of antioxidant defence, reacts with $O_2\cdot^-$ to produce H_2O_2, while CAT, an H_2O_2 scavenging enzyme, breaks down H_2O_2 and prevents it from accumulating in the cell [64]. Gohari [65], Cai [66] and Ji [31] found that SOD, POD and CAT activities in *Vitis vinifera* L., *Lonicera japonica* Thunb. and *Juglans regia* L. tended to increase and then decrease under saline–alkali stress conditions, respectively. However, our results differed in that SOD, CAT and POD activities tended to increase with the increasing saline–alkali gradient. It was shown that the synthesis of antioxidant enzymes in the cells of Hotan Red leaves was not affected within the range of saline–alkali stress treatments in this experiment, and the biomolecules, such as DNA, proteins and membrane systems, were protected by the continuous enhancement of antioxidant enzyme activities, which then maintained the normal physiological functions of the cells.

Saline–alkali stress leads to increased levels of ROS in plant cells, and if the ROS scavenging mechanism is not able to balance this, it will lead to a large accumulation of ROS, such as H_2O_2 and $O_2\cdot^-$, which in turn attack cell membrane lipids, proteins and nucleic acids, triggering programmed cell death and leading to an increase in the saline–alkali index of the plant [67,68]. It is noteworthy that the results of the present

study, when considered alongside the partial least squares path model (PLS-PM) analysis, indicate that photosynthetic parameters represent the primary drivers of the saline–alkali damage index of Hotan Red, with oxidation product and antioxidant enzyme parameters and chlorophyll fluorescence parameters exerting a lesser influence. Conversely, there is no direct relationship between osmoregulatory substances and the saline–alkali damage index. Furthermore, there were strong correlations ($R > 0.85$) between osmoregulatory substances, oxidation products and antioxidant enzyme systems, chlorophyll fluorescence parameters and photosynthetic parameters, respectively. These findings indicate that the index of saline–alkali damage in Hotan Red is directly influenced by photosynthesis, ROS accumulation and antioxidant enzyme activities, with an indirect correlation with osmoregulatory substances. There are two possible reasons for this phenomenon: (a) the weakening of photosynthetic carbon assimilation triggered the accumulation of ROS, and the excessive ROS led to the occurrence of photo-oxidation in photosynthetic organs, resulting in the disturbance of the photosynthetic system, affecting the normal growth and metabolism of the plant, and ultimately leading to the loss of the green colour of the leaves, abscission and other phenotypic changes. (b) Excess Na^+ and high pH limit cellular uptake of, for example, Fe^{2+} and Mg^{2+}, which affects chlorophyll synthesis and the stability of photosynthetic electron transport, leading to a reduction in photosynthetic efficiency. As a result, the energy and reducing power of the cell are insufficient, which affects the normal physiological function of the cell and induces programmed cell death.

5. Conclusions

In this study, the growth, physiological and biochemical responses of Xinjiang native grapevine germplasm Hotan Hong were investigated under different gradients of combined saline–alkali stress (0, 40, 80, 120 and 160 mmol·L^{-1}). The results showed that the growth of plant height and shoot diameter of Hotan Red was inhibited under saline–alkali stress, and the saline–alkali damage index increased, indicating that the leaves lost green colour, wilted and dropped. In addition, the non-stomatal restriction of Hotan Red led to the inhibition of photosynthesis, mainly manifested as decreases in *Pn*, *Tr*, *Gs*, an increase in *Ci*, structural changes in the PSII reaction centre or dysfunction ($\varphi PSII$ and F_v/F_m decreased). The accumulation of MDA, $O_2\cdot^-$ and H_2O_2 levels and the increase in REC reflected the apparent damage caused by lipid peroxidation and cellular oxidation. This suggests that, although Hotan Red activates antioxidant mechanisms such as the increased activity of antioxidant enzymes (SOD, CAT and POD) and the accumulation of osmoregulatory substances (Pro, SS and SP), the clearance rate of antioxidant mechanisms cannot be balanced with the accumulation of ROS. Furthermore, PLS-PM analysis of the above variables showed that photosynthesis was the main driver of the saline–alkali damage index in Hotan Red, followed by oxidation products and antioxidant enzymes, while osmoregulatory substances had an indirect effect.

Author Contributions: Conceptualization, L.Z. and Y.S.; methodology, R.L.; formal analysis, R.L., L.J. and X.W.; investigation, L.J.; writing—original draft preparation, Y.S.; writing—review and editing, Y.S. and L.Z. All authors have read and agreed to the published version of the manuscript.

Funding: Xinjiang Natural Science Foundation of Xinjiang Uygur Autonomous Region (2022D01A179).

Data Availability Statement: The original contributions presented in this study are included in the article. Further inquiries can be directed to the corresponding author.

Conflicts of Interest: The authors declare no conflicts of interest.

References

1. Sun, Z.; Liu, W.; Zheng, X.; Zheng, X.; Gong, X.; Ma, C.; Liu, X.; Wang, C.; Tian, Y. Effects and Functional Mechanism of Melatonin on the Growth of *Malus hupehensis* Seedlings Under Saline-Alkali Stress. *Acta Hortic. Sin.* **2023**, *50*, 1697–1710. [CrossRef]
2. Lim, S.J.; Shin, M.N.; Son, J.K.; Song, J.D.; Cho, J.Y. Evaluation of soil pore-water salinity using a Decagon GS3 sensor in saline-alkali reclaimed tidal lands. *Comput. Electron. Agric.* **2017**, *132*, 49–55. [CrossRef]
3. Wei, B. Distribution and genetic analysis of saline-alkali soil in China. *Technol. Soil Water Conserv.* **2012**, *6*, 27–28.
4. Guo, R.; Yang, Z.; Li, F.; Yan, C.; Zhong, X.; Liu, Q.; Xia, X.; Li, H.; Zhao, L. Comparative metabolic responses and adaptive strategies of wheat (*Triticum aestivum*) to salt and alkali stress. *BMC Plant Biol.* **2015**, *15*, 170. [CrossRef]
5. Song, L.; Yu, Y.; Chen, H.; Feng, Y.; Chen, S.; Zhang, H.; Zhou, H.; Meng, L.; Wang, Y. Response of photosynthetic characteristics and antioxidant system in the leaves of safflower to NaCl and $NaHCO_3$. *Plant Cell Rep.* **2024**, *43*, 146. [CrossRef]
6. Pang, Q.; Zhang, A.; Zang, W.; Wei, L.; Yan, X. Integrated proteomics and metabolomics for dissecting the mechanism of global responses to salt and alkali stress in *Suaeda corniculata*. *Plant Soil* **2016**, *402*, 379–394. [CrossRef]
7. Yin, Z.; Zhang, H.; Zhao, Q.; Yoo, M.J.; Zhu, N.; Yu, J.; Yu, J.; Guo, S.; Miao, Y.; Chen, S.; et al. Physiological and comparative proteomic analyses of saline-alkali $NaHCO_3$-responses in leaves of halophyte *Puccinellia tenuiflora*. *Plant Soil* **2019**, *437*, 137–158. [CrossRef]
8. Chen, S.; Zhou, Q.; Feng, Y.; Dong, Y.; Zhang, Z.; Wang, Y.; Liu, W. Responsive mechanism of *Hemerocallis citrina* Baroni to complex saline-alkali stress revealed by photosynthetic characteristics and antioxidant regulation. *Plant Cell Rep.* **2024**, *43*, 176. [CrossRef]
9. Zhao, Q.; Chen, S.; Wang, G.; Du, Y.; Zhang, Z.; Yu, G.; Ren, C.; Zhang, Y.; Du, J. Exogenous melatonin enhances soybean (*Glycine max* (L.) Merr.) seedling tolerance to saline-alkali stress by regulating antioxidant response and DNA damage repair. *Physiol. Plant.* **2022**, *174*, e13731. [CrossRef]
10. Wang, X.; Chen, Z.; Sui, N. Sensitivity and responses of chloroplasts to salt stress in plants. *Front. Plant Sci.* **2024**, *15*, 1374086. [CrossRef]
11. Zargar, S.M.; Zargar, M.Y. *Abiotic Stress-Mediated Sensing and Signaling in Plants: An Omics Perspective* | | *Multifarious Role of ROS in Halophytes: Signaling and Defense*; Springer: Berlin/Heidelberg, Germany, 2018; pp. 207–223. [CrossRef]
12. Rangani, J.; Parida, A.K.; Panda, A.; Kumari, A. Coordinated Changes in Antioxidative Enzymes Protect the Photosynthetic Machinery from Salinity Induced Oxidative Damage and Confer Salt Tolerance in an Extreme Halophyte *Salvadora persica* L. *Front. Plant Sci.* **2016**, *7*, 50. [CrossRef] [PubMed]
13. Zhang, X.; Li, S.; Tang, T.; Liu, Y.; Mobeen, T.M.; Wang, C.; Meng, Z.; Niu, J.; Yang, W.; Ma, J. Comparison of morphological, physiological, and related-gene expression responses to saline-alkali stress in eight apple rootstock genotypes. *Sci. Hortic.* **2022**, *306*, 111455. [CrossRef]
14. Zhong, Y.; Qi, X.; Chen, J.; Li, Z.; Bai, D. Growth and physiological responses of four kiwifruit genotypes to salt stress and resistance evaluation. *J. Integr. Agric.* **2019**, *18*, 87–99. [CrossRef]
15. Wei, J.; Liu, D.; Liu, Y.; Wei, S. Physiological Analysis and Transcriptome Sequencing Reveal the Effects of Salt Stress on Banana (*Musa acuminata* cv. BD) Leaf. *Front. Plant Sci.* **2022**, *13*, 822838. [CrossRef]
16. Boughalleb, F.; Abdellaoui, R.; Mahmoudi, M.; Bakhshandeh, E. Changes in phenolic profile, soluble sugar, proline, and antioxidant enzyme activities of Polygonumequisetiforme in response to salinity. *Turk. J. Bot.* **2020**, *44*, 25–35. [CrossRef]
17. Amini, F.; Ehsanpour, A.A. Soluble Proteins, Proline, Carbohydrates and Na^+/K^+ Changes in Two Tomato (*Lycopersicon esculentum* Mill.) Cultivars under in vitro Salt Stress. *Am. J. Biochem. Biotechnol.* **2005**, *1*, 212–216. [CrossRef]
18. Ma, Y.; Riziwangguli, A.; Bai, S.; Zhong, H.; Zhang, F.; Hu, J.; Wu, X.; Wu, J. Analyze on development of grape industry in Xinjiang. *China Fruits* **2024**, *9*, 102–108. [CrossRef]
19. Zhao, J.; Ma, L.; Zhang, Y.; Bahar, G. An experimental study of antitumor effects on Xinjiang Hotan Red grape in vitro. *J. Xinjiang Med. Univ.* **2001**, *2*, 95–97.
20. Wang, F.; Yang, S.; Wei, Y.; Shi, Q.; Ding, J. Characterizing soil salinity at multiple depth using electromagnetic induction and remote sensing data with random forests: A case study in Tarim River Basin of southern Xinjiang, China. *Sci. Total Environ.* **2021**, *754*, 142030. [CrossRef]
21. Du, Z.; Zhai, H.; Luo, X.; Pan, Z.; Cheng, S. Salt-Tolerance Identification on Apple Rootstocks. *J. Fruit Sci.* **2002**, *1*, 4–7. [CrossRef]
22. Hussain, S.; Huang, J.; Zhu, C.; Zhu, L.; Cao, X.; Hussain, S.; Ashraf, M.; Khaskheli, M.A.; Kong, Y.; Jin, Q.; et al. Pyridoxal 5′-phosphate enhances the growth and morpho-physiological characteristics of rice cultivars by mitigating the ethylene accumulation under salinity stress. *Plant Physiol. Biochem.* **2020**, *154*, 782–795. [CrossRef] [PubMed]
23. Zhao, Y.; Jia, K.; Tian, Y.; Han, K.; El-Kassaby, Y.A.; Yang, H.; Si, H.; Sun, Y.; Li, Y. Time-course transcriptomics analysis reveals key responses of populus to salt stress. *Ind. Crop. Prod.* **2023**, *194*, 116278. [CrossRef]
24. Vieira, S.M.A.; Silva, T.M.; Glória, M.B.A. Influence of processing on the levels of amines and proline and on the physicochemical characteristics of concentrated orange juice. *Food Chem.* **2010**, *119*, 7–11. [CrossRef]

25. Campion, E.M.; Walls, D.; Loughran, S.T. Protein Quantitation and Analysis of Purity. *Methods Mol. Biol.* **2023**, *2699*, 305–347. [CrossRef]
26. Wang, L.; Wang, Y.; Wang, X.; Li, Y.; Peng, F.; Wang, L. Regulation of POD activity by pelargonidin during vegetative growth in radish (*Raphanus sativus* L.). *Sci. Hortic.* **2014**, *174*, 105–111. [CrossRef]
27. Song, Y.; Zhang, R.; Gao, S.; Pan, Z.; Guo, Z.; Yu, S.; Wang, Y.; Jin, Q.; Chen, X.; Zhang, L. Transcriptome analysis and phenotyping of walnut seedling roots under nitrogen stresses. *Sci. Rep.* **2022**, *12*, 12066. [CrossRef]
28. Zhang, H.; Zhao, Y.; Zhu, J.K. Thriving under Stress: How Plants Balance Growth and the Stress Response. *Dev. Cell* **2020**, *55*, 529–543. [CrossRef]
29. Yu, X.; Yue, Q.; Yu, M.; Du, Y.; Yao, Y. Physiological responses of grape rootstocks SA15, SA17 and 1103P to salt-alkali stress. *Plant Physiol. J.* **2020**, *56*, 57–65. [CrossRef]
30. Lu, Y.; Li, M.; Chen, X. Effect of saline-alkali stress on the growth and related physiological indicators of 'Cabernet Sauvignon' grape seedlings. *Acta Bot. Boreali-Occident. Sin.* **2024**, *44*, 182–193.
31. Ji, X.; Tang, J.; Zhang, J. Effects of Salt Stress on the Morphology, Growth and Physiological Parameters of *Juglansmicrocarpa* L. Seedlings. *Plants* **2022**, *11*, 2381. [CrossRef]
32. Xu, J.; Sui, C.; Ge, J.; Ren, R.; Pang, Y.; Gan, H.; Du, Y.; Cao, H.; Sun, Q. Exogenous spermidine improved the salinity-alkalinity stress tolerance of grapevine (*Vitis vinifera*) by regulating antioxidant system, Na^+/K^+ homeostasis and endogenous polyamine contents. *Sci. Hortic.* **2024**, *326*, 112725. [CrossRef]
33. Qin, L.; Kang, W.; Qi, Y.; Cai, A. Effects of Salt Stress on Mesophyll Cell Structures and Photosynthetic Characteristics in Leaves of Wine Grape (*Vitis* spp.). *Sci. Agric. Sin.* **2012**, *45*, 4233–4241.
34. Xiong, H.; Tian, X.; Mao, P.; Zheng, L.; Fu, J.; Meng, L. Effects of Exogenous Melatonin on Photosynthetic and Physiological Characteristics of White Clover Seedlings under Salt Stress. *Pratacultural Sci.* **2024**, 1–20.
35. Wang, W.; Gao, L.; Zhang, R.; Zhao, T.; Zhang, Z.; Wang, S.; Wang, Y. Effects of 2,4 ep brassinolide on photosynthetic and physiological characteristics of *Malusa halliana* under saline-alkali stress. *J. Fruit Sci.* **2021**, *38*, 1479–1490. [CrossRef]
36. Lu, Q.; Chen, L.; Ma, Y.; Liu, Y.; Zhao, Y.; Zhao, B.; Sun, J. Effects of saline-alkali stress on photosynthetic and chlorophyll fluorescence characteristics of different grape rootstocks. *J. Fruit Sci.* **2022**, *39*, 773–783. [CrossRef]
37. Niu, M.; Xie, J.; Chen, C.; Cao, H.; Sun, J.; Kong, Q.; Shabala, S.; Shabala, L.; Huang, Y.; Bie, Z. An early ABA-induced stomatal closure, Na^+ sequestration in leaf vein and K^+ retention in mesophyll confer salt tissue tolerance in Cucurbita species. *J. Exp. Bot.* **2018**, *69*, 4945–4960. [CrossRef]
38. Geilfus, C.M.; Mithöfer, A.; Ludwig-Müller, J.; Zörb, C.; Muehling, K.H. Chloride-inducible transient apoplastic alkalinizations induce stomata closure by controlling abscisic acid distribution between leaf apoplast and guard cells in salt-stressed *Vicia faba*. *New Phytol.* **2015**, *208*, 803–816. [CrossRef]
39. Hasanuzzaman, M.; Shabala, L.; Zhou, M.; Brodribb, T.J.; Corkrey, R.; Shabala, S. Factors determining stomatal and non-stomatal (residual) transpiration and their contribution towards salinity tolerance in contrasting barley genotypes. *Environ. Exp. Bot.* **2018**, *153*, 10–20. [CrossRef]
40. Nefissi, O.R.; Arasappan, D.; Ruhlman, T.A.; Ben, C.M.; Abid, G.; Mejri, S.; Ghorbel, A.; Jansen, R.K. Effects of Salt Stress on Transcriptional and Physiological Responses in Barley Leaves with Contrasting Salt Tolerance. *Int. J. Mol. Sci.* **2022**, *23*, 5006. [CrossRef]
41. Abdelgawad, H.; Zinta, G.; Hegab, M.M.; Pandey, R.; Asard, H.; Abuelsoud, W. High Salinity Induces Different Oxidative Stress and Antioxidant Responses in Maize Seedlings Organs. *Front. Plant Sci.* **2016**, *7*, 276. [CrossRef]
42. Martin, R.B.F. Rootstocks increase grapevine tolerance to NaCl through ion compartmentalization and exclusion. *Acta Physiol. Plant* **2020**, *42*, 1–11. [CrossRef]
43. Song, C.; Dong, S.; Schlisser, A.; Lupo, Y.; Rachmilevitch, S.; Lazarovitch, N.; Fait, A. Rootstock varietal ability in accumulation of chloride ions underpins improved physiology and metabolism of grapevine exposed to salinity. *Sci. Hortic.* **2024**, *328*, 112964. [CrossRef]
44. Zhu, Y.; Wu, Y.; Hu, Y.; Jia, X.; Zhao, T.; Cheng, L.; Wang, Y. Tolerance of two apple rootstocks to short-term salt stress: Focus on chlorophyll degradation, photosynthesis, hormone and leaf ultrastructures. *Acta Physiol. Plant* **2019**, *41*, 1–14. [CrossRef]
45. Shankar, K.; Awasthi, O.P.; Dubey, A.K. Rootstock mediated alteration in morphology and photosystem in sweet orange (*Citrus sinensis*) scion cv. Pusa Sharad under NaCl stress. *Indian J. Agric. Sci.* **2023**, *93*, 1103–1107. [CrossRef]
46. Stefanov, M.A.; Rashkov, G.D.; Apostolova, E.L. Assessment of the Photosynthetic Apparatus Functions by Chlorophyll Fluorescence and P_{700} Absorbance in C3 and C4 Plants under Physiological Conditions and under Salt Stress. *Int. J. Mol. Sci.* **2022**, *23*, 3768. [CrossRef]
47. Moustakas, M. Harnessing Chlorophyll Fluorescence for Phenotyping Analysis of Wild and Cultivated Tomato for High Photochemical Efficiency under Water Deficit for Climate Change Resilience. *Climate* **2021**, *9*, 154. [CrossRef]
48. Zhao, J.; Li, Q.; Lu, B.; Wang, M.; Li, Y.; Lu, B. Comparison of Photosynthetic Parameters Between *Pyrus betulaefolia* and *Pyrus calleryana* Under NaCl Stress. *North. Hortic.* **2019**, *22*, 97–104.

49. Galicia-Campos, E.; Garcia-Villaraco, A.; Montero-Palmero, M.B.; Gutierrez-Manero, F.J.; Ramos-Solano, B. Bacillus G7 improves adaptation to salt stress in *Olea europaea* L. plantlets, enhancing water use efficiency and preventing oxidative stress. *Sci. Rep.* **2023**, *13*, 22507. [CrossRef]
50. Lu, X.; Ma, L.; Zhang, C.; Yan, H.; Bao, J.; Gong, M.; Wang, W.; Li, S.; Ma, S.; Chen, B. Grapevine (*Vitis vinifera*) responses to salt stress and alkali stress: Transcriptional and metabolic profiling. *Bmc Plant Biol.* **2022**, *22*, 528. [CrossRef]
51. Liu, B.; Wang, X.; Li, K.; Cai, Z. Spatially Resolved Metabolomics and Lipidomics Reveal Salinity and Drought-Tolerant Mechanisms of Cottonseeds. *J. Agric. Food Chem.* **2021**, *69*, 8028–8037. [CrossRef]
52. Meena, M.; Divyanshu, K.; Kumar, S.; Swapnil, P.; Zehra, A.; Shukla, V.; Yadav, M.; Upadhyay, R.S. Regulation of L-proline biosynthesis, signal transduction, transport, accumulation and its vital role in plants during variable environmental conditions. *Heliyon* **2019**, *5*, e02952. [CrossRef] [PubMed]
53. Sharma, A.; Shahzad, B.; Kumar, V.; Kohli, S.K.; Sidhu, G.; Bali, A.S.; Handa, N.; Kapoor, D.; Bhardwaj, R.; Zheng, B. Phytohormones Regulate Accumulation of Osmolytes Under Abiotic Stress. *Biomolecules* **2019**, *9*, 285. [CrossRef] [PubMed]
54. Chen, Z.; Shi, X.; Wang, R.; Wu, X.; Wang, N.; Wang, Z. Osmotic Regulation and Antioxidant Capacity of Different Grapevine Rootstocks under Salt Stress. *Acta Bot. Boreali-Occident. Sin.* **2022**, *42*, 1880–1891.
55. Oliveira, L.M.; Mendonca, V.; Moura, E.A.; Irineu, T.; Figueiredo, F.; Melo, M.F.; Celedonio, W.F.; Rego, A.; Mendonca, L.; Andrade, A. Salt stress and organic fertilization on the growth and biochemical metabolism of *Hylocereus costaricensis* (red pitaya) seedlings. *Braz. J. Biol.* **2022**, *84*, e258476. [CrossRef]
56. Guo, X.; Ahmad, N.; Zhao, S.; Zhao, C.; Zhong, W.; Wang, X.; Li, G. Effect of Salt Stress on Growth and Physiological Properties of Asparagus Seedlings. *Plants* **2022**, *11*, 2836. [CrossRef]
57. Xu, X.; Zhang, J.; Yan, B.; Wei, Y.; Ge, S.; Li, J.; Han, Y.; Li, Z.; Zhao, C.; Xu, J. The Adjustment of Membrane Lipid Metabolism Pathways in Maize Roots Under Saline-Alkaline Stress. *Front. Plant Sci.* **2021**, *12*, 635327. [CrossRef]
58. Zhang, H.; Liu, X.; Zhang, R.; Yuan, H.; Wang, M.; Yang, H.; Ma, H.; Liu, D.; Jiang, C.; Liang, Z. Root Damage under Alkaline Stress Is Associated with Reactive Oxygen Species Accumulation in Rice (*Oryza sativa* L.). *Front. Plant Sci.* **2017**, *8*, 1580. [CrossRef]
59. Li, H.; Guo, X. Influence of NaCl on activities of protective enzymes and MDA content in grape rootstock leaves. *J. Fruit Sci.* **2008**, *25*, 240–243.
60. Bonnin, M.; Favreau, B.; Soriano, A.; Leonhardt, N.; Oustric, J.; Lourkisti, R.; Ollitrault, P.; Morillon, R.; Berti, L.; Santini, J. Insight into Physiological and Biochemical Determinants of Salt Stress Tolerance in Tetraploid Citrus. *Antioxidants* **2023**, *12*, 1640. [CrossRef]
61. Wang, D.; Gao, Y.; Sun, S.; Lu, X.; Li, Q.; Li, L.; Wang, K.; Liu, J. Effects of Salt Stress on the Antioxidant Activity and Malondialdehyde, Solution Protein, Proline, and Chlorophyll Contents of Three Malus Species. *Life* **2022**, *12*, 1929. [CrossRef]
62. Tirani, M.M.; Haghjou, M.M. Reactive oxygen species (ROS), Total antioxidant capacity (AOC) and Malondialdehyde (MDA) make a triangle in the evaluation of Zinc stress extension. *J. Anim. Plant Sci.* **2019**, *29*, 1100–1111.
63. Tan, W.; Li, X.; Dong, Z.; Tan, M.; Tang, X. Principal component analysis on the alleviating effects of different concentrations of $CaCl_2$ on 'Tamina' grape under NaCl stress. *Plant Physiol. J.* **2018**, *54*, 574–580. [CrossRef]
64. Peng, Z.; Wang, Y.; Geng, G.; Yang, R.; Yang, Z.; Yang, C.; Xu, R.; Zhang, Q.; Kakar, K.U.; Li, Z.; et al. Comparative Analysis of Physiological, Enzymatic, and Transcriptomic Responses Revealed Mechanisms of Salt Tolerance and Recovery in Tritipyrum. *Front. Plant Sci.* **2021**, *12*, 800081. [CrossRef] [PubMed]
65. Gohari, G.; Zareei, E.; Rostami, H.; Panahirad, S.; Kulak, M.; Farhadi, H.; Amini, M.; Martinez-Ballesta, M.; Fotopoulos, V. Protective effects of cerium oxide nanoparticles in grapevine (*Vitis vinifera* L.) cv. Flame Seedless under salt stress conditions. *Ecotox Environ. Safe* **2021**, *220*, 112402. [CrossRef]
66. Cai, Z.; Liu, X.; Chen, H.; Yang, R.; Chen, J.; Zou, L.; Wang, C.; Chen, J.; Tan, M.; Mei, Y.; et al. Variations in morphology, physiology, and multiple bioactive constituents of Lonicerae Japonicae Flos under salt stress. *Sci. Rep.* **2021**, *11*, 3939. [CrossRef]
67. Lin, J.; Wang, Y.; Wang, G. Salt stress-induced programmed cell death in tobacco protoplasts is mediated by reactive oxygen species and mitochondrial permeability transition pore status. *J. Plant Physiol.* **2006**, *163*, 731–739. [CrossRef]
68. Hasanuzzaman, M.; Raihan, M.; Masud, A.; Rahman, K.; Nowroz, F.; Rahman, M.; Nahar, K.; Fujita, M. Regulation of Reactive Oxygen Species and Antioxidant Defense in Plants under Salinity. *Int. J. Mol. Sci.* **2021**, *22*, 9326. [CrossRef]